ADVANCED MATERIALS

Supporting Information

for *Adv. Mater.*, DOI: 10.1002/adma.201506234

Intrinsically Stretchable Biphasic (Solid–Liquid) Thin Metal Films

*Arthur Hirsch, Hadrien O. Michaud, Aaron P. Gerratt, Séverine de Mulatier, and Stéphanie P. Lacour**

Supporting Information should be included here (for submission only; for publication, please provide Supporting Information as a separate PDF file).

Supplementary Information

Intrinsically stretchable biphasic (solid-liquid) thin metal films

Arthur Hirsch[†], Hadrien O. Michaud[†], Aaron P. Gerratt, Séverine de Mulatier, Stéphanie P. Lacour[*]

1. Supplementary Figures
2. Supplementary Methods
3. Supplementary Note
4. Supplementary Movies

1. List of Supplementary Figures

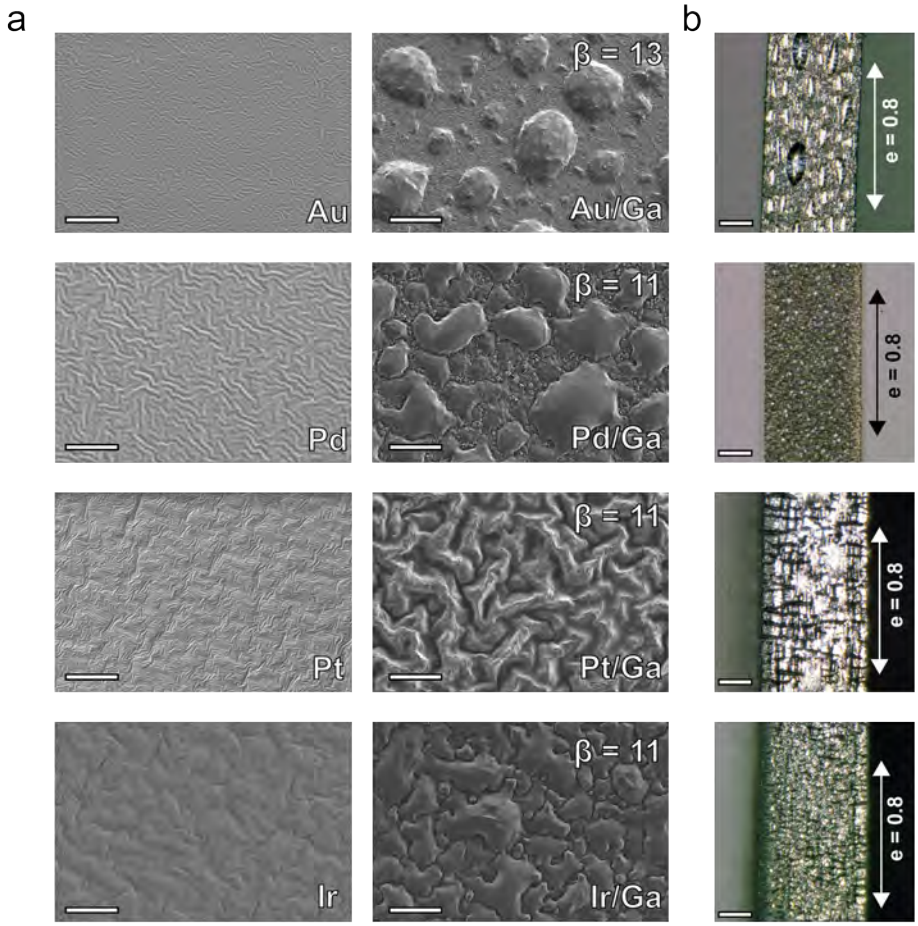

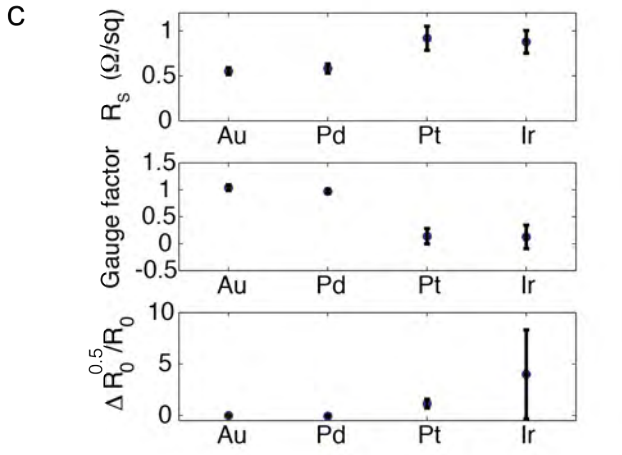

Supplementary Figure S1: Electromechanical characterization of biphasic gallium-based thin films on PDMS substrates. a, SEM images of the surface of films after sputter deposition of the 60 nm metal layer on a PDMS substrate (left) and after the subsequent gallium thermal evaporation (right). Scale bars are 20 µm. **b,** Optical microscope images of 300 µm wide tracks of the biphasic films under 0.8 applied mechanical strain. Scale bars are 100 µm. **c,** Sheet resistance, gauge factor and relative change in baseline resistance at zero strain after the tracks were stretched to 0.5 strain. Corresponding atomic ratios n_{metal}/n_{Ga} β are 13 for Au, 11 for Pt, 11 for Pt and 11 for Ir. (n = 4 for each data point, error bars: S.D.).

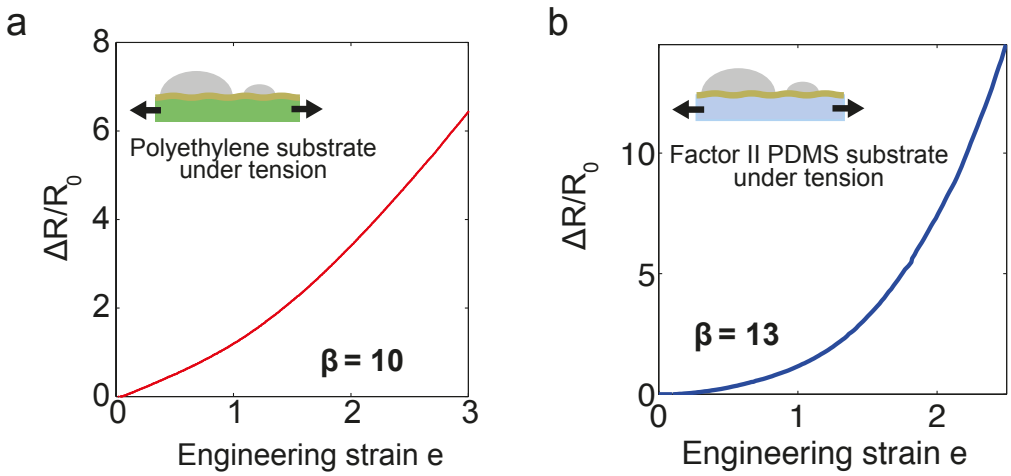

Supplementary Figure S2: Electromechanical response of biphasic gold-gallium thin film conductors on plastic and elastomer substrates. a, Relative resistance change as a function of engineering strain *e* for a gold-gallium biphasic film deposited on a 10 µm thin polyethylene substrate (Ideal from Weita) with the atomic ratio n_{Ga}/n_{Au} β = 10. Initial sheet resistance of the sample was 0.6 Ω/sq. **b,** Relative resistance change as a function of engineering strain *e* for an gold-gallium biphasic film deposited on a 120 µm thin PDMS substrate (A-221-05 from Factor II) with the atomic ratio n_{Ga}/n_{Au} β = 13. Initial sheet resistance of the sample was 0.6 Ω/sq.

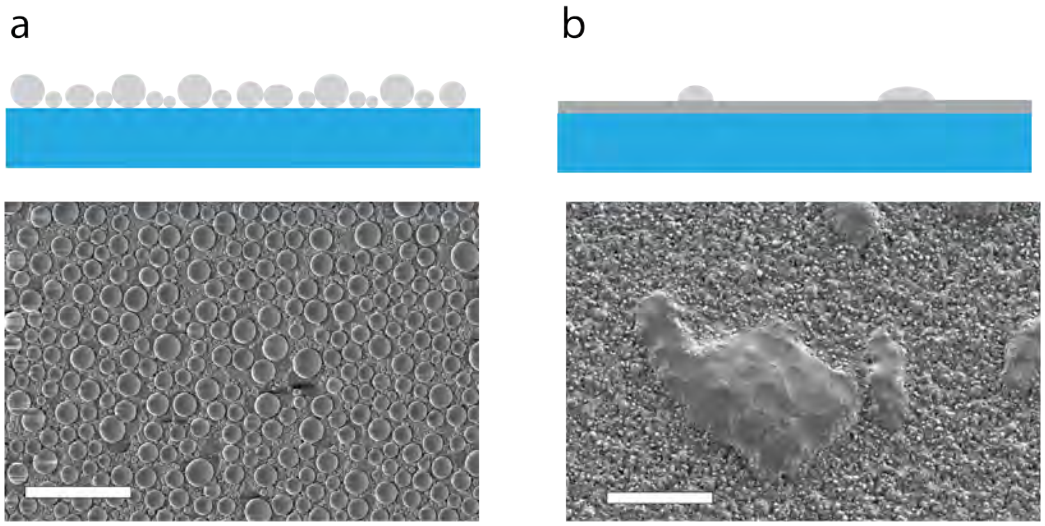

Supplementary Figure S3: Thermal evaporation of gallium on bare and gold-coated PDMS substrates. **a,** Schematic (top) and scanning electron microscope image (bottom) of gallium deposited by thermal evaporation on a bare PDMS substrate. The evaporated gallium condensed on the substrate to form a non-percolating layer of micro-droplets. Scale bar is 5 µm. **b,** Schematic (top) and scanning electron microscope image (bottom) of gallium deposited by thermal evaporation on PDMS substrate previously coated with sputtered gold (60 nm in thickness). The thin gold coating allows the gallium to spread by diffusing and alloying. Scale bar is 5 µm.

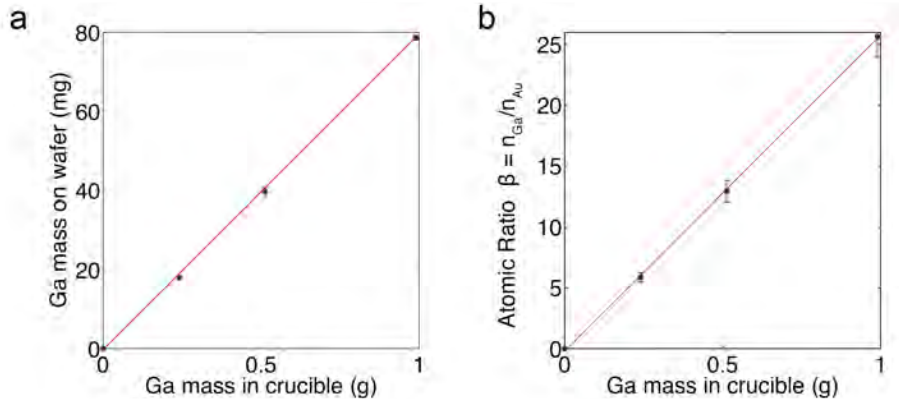

Supplementary Figure S4: Calibration of gallium evaporation and computation of the Ga/Au atomic ratio β. a, Gallium mass on glass wafers coated with 60 nm of sputtered gold as a function of gallium mass introduced in the crucible of the thermal evaporator. Masses were measured using a PB303-L precision scale from Mettler Toledo (n = 3 for each point, error bars: S.D.). **b,** Corresponding Ga/Au atomic ratio β derived from the mass of sputtered gold (8.7 ± 0.5 mg, mean ± S.D., n = 3). Red line represents linear fit.

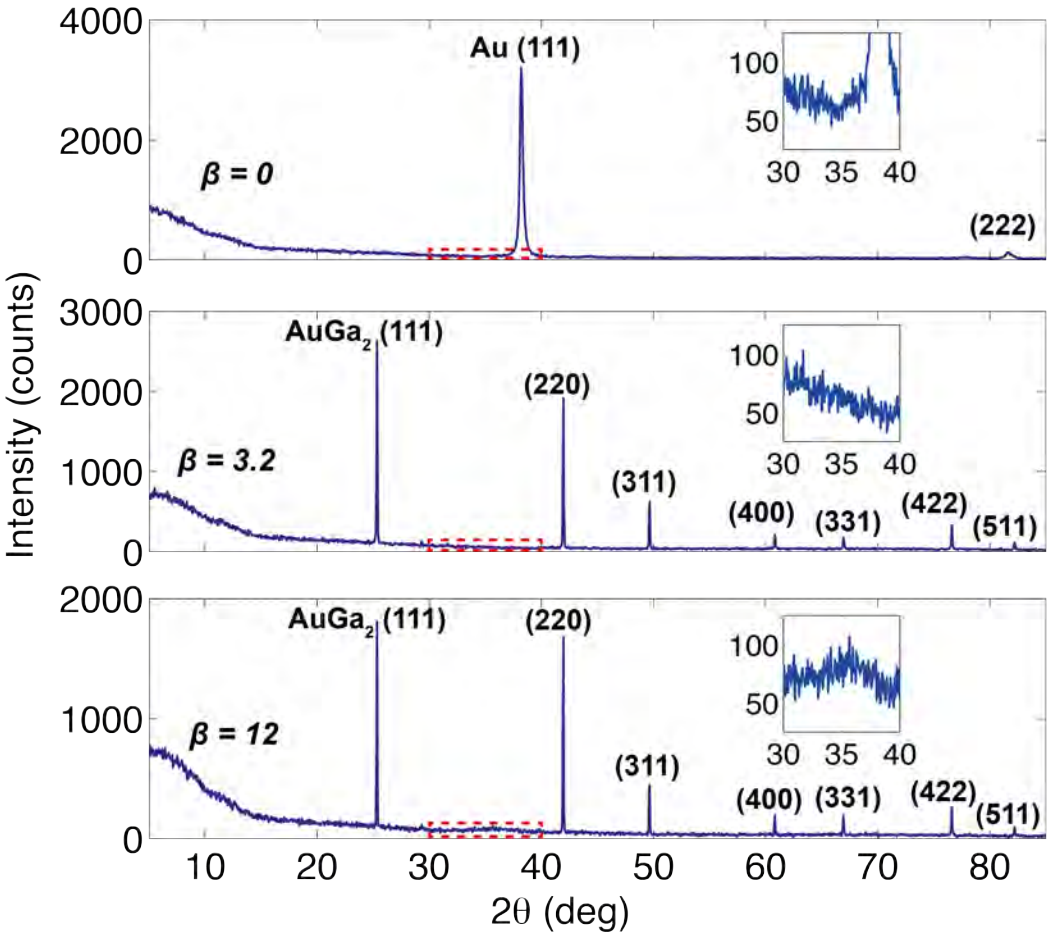

Supplementary Figure S5: X-Ray diffraction analysis of biphasic gold-gallium thin film. All samples were prepared by spin-coating a 120 µm thick PDMS layer on a float glass wafer. The PDMS was then coated with 60 nm of sputtered Au and a controlled amount of Ga was evaporated to form the biphasic gold-gallium film. We identified the peaks corresponding to Au (for β = 0, ICDD PDF Card 00-004-0784) and $AuGa_2$ (for β = 3.2 and β = 12, ICDD PDF Card 01-072-5268). Insets show the increase in baseline signal around 35° attributed to liquid gallium.

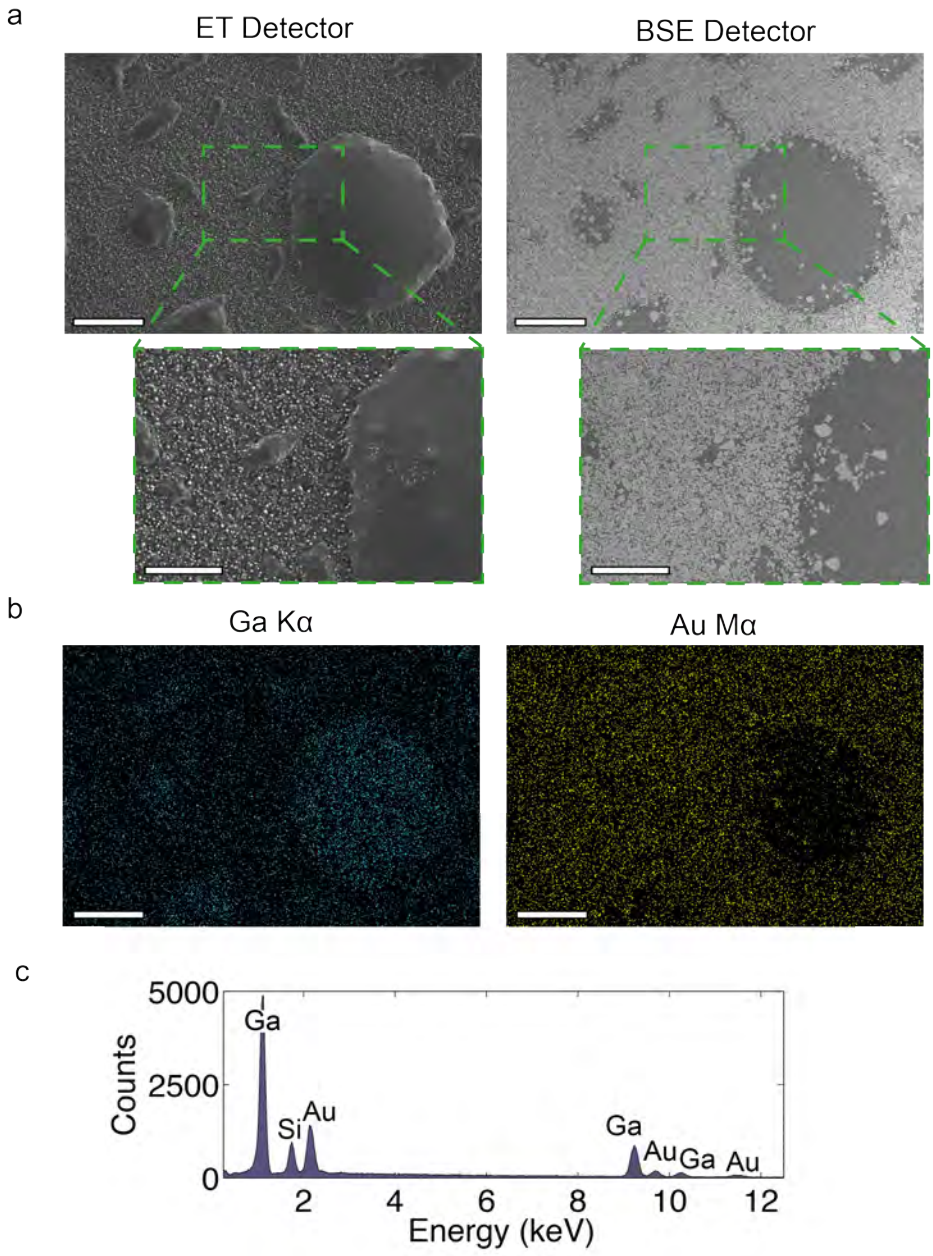

Supplementary Figure S6: EDS-SEM analysis of the gold-gallium films. **a,** SEM images of the surface of a biphasic gold-gallium thin film deposited on a PDMS substrate with Ga/Au atomic ratio β = 13. Left-hand images were acquired with an Everhart-Thornley (ET) detector. Right-hand images were acquired using a backscattered electron (BSE) detector. Scale bars are 10 µm (5 µm in the magnified views). **b,** Energy-dispersive X-Ray spectroscopy (EDS) mapping of the area observed in **a** for gold and gallium. Scale bars are 10 µm. **c,** EDS spectrum corresponding to the mapping shown in **b**.

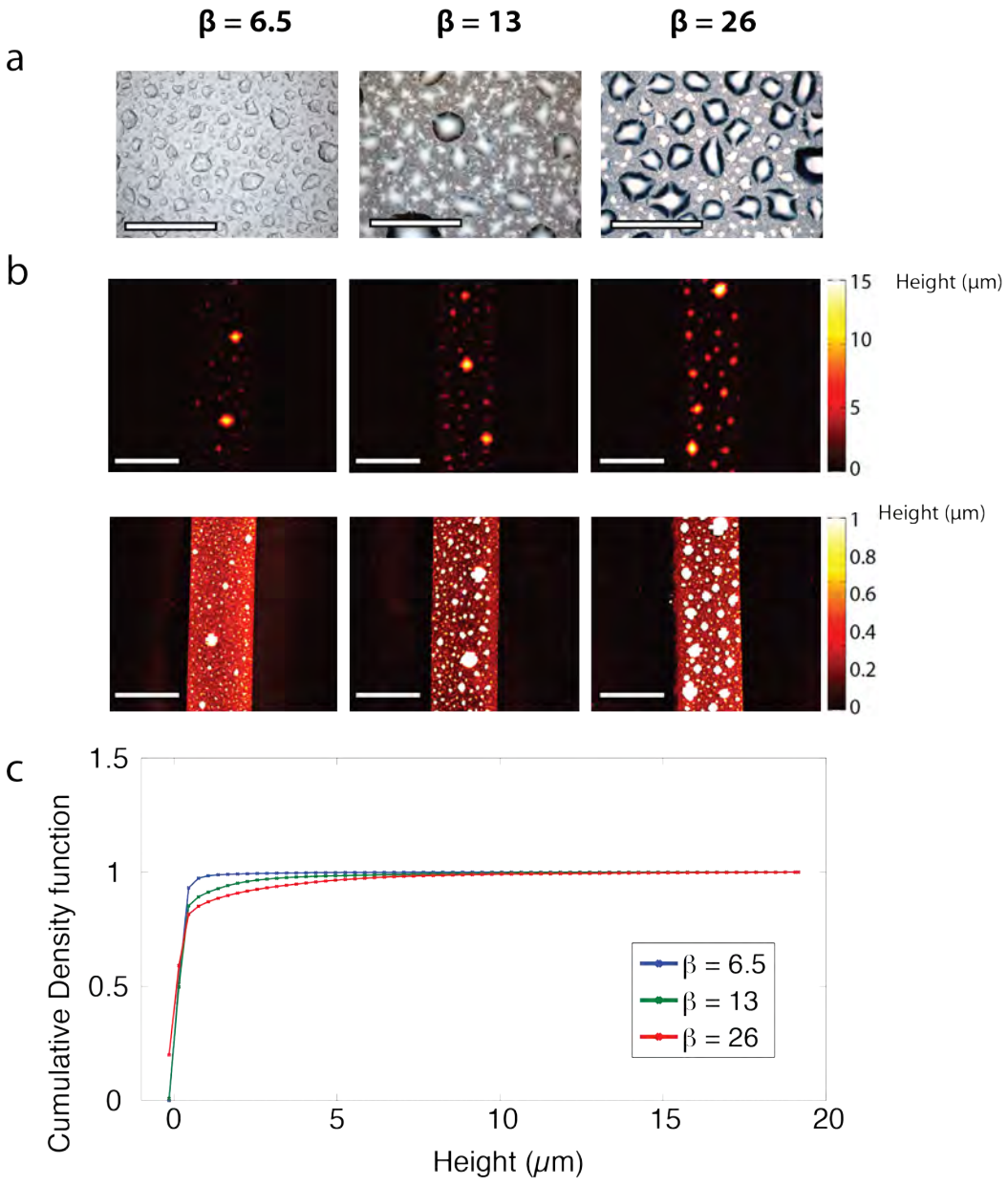

Supplementary Figure S7: Surface profiles of biphasic gold-gallium thin films on PDMS substrates. **a,** Microscope images of biphasic gold-gallium thin films on PDMS substrates for different atomic ratio β. Scale bars are 100 μm. **b,** Topology of a 300 μm wide biphasic thin film traces on PDMS substrates measured using phase shifting optical profilometry (Wyko NT1100). The top three images are displayed using color scale from 0 to 15 μm. The bottom three images are displayed using color scale ranging from 0 to 1 μm to emphasize the thin region of the films. Scale bar are 300 μm. **c,** Cumulative height distribution functions of the biphasic thin films on PDMS substrates for increasing atomic ratio β.

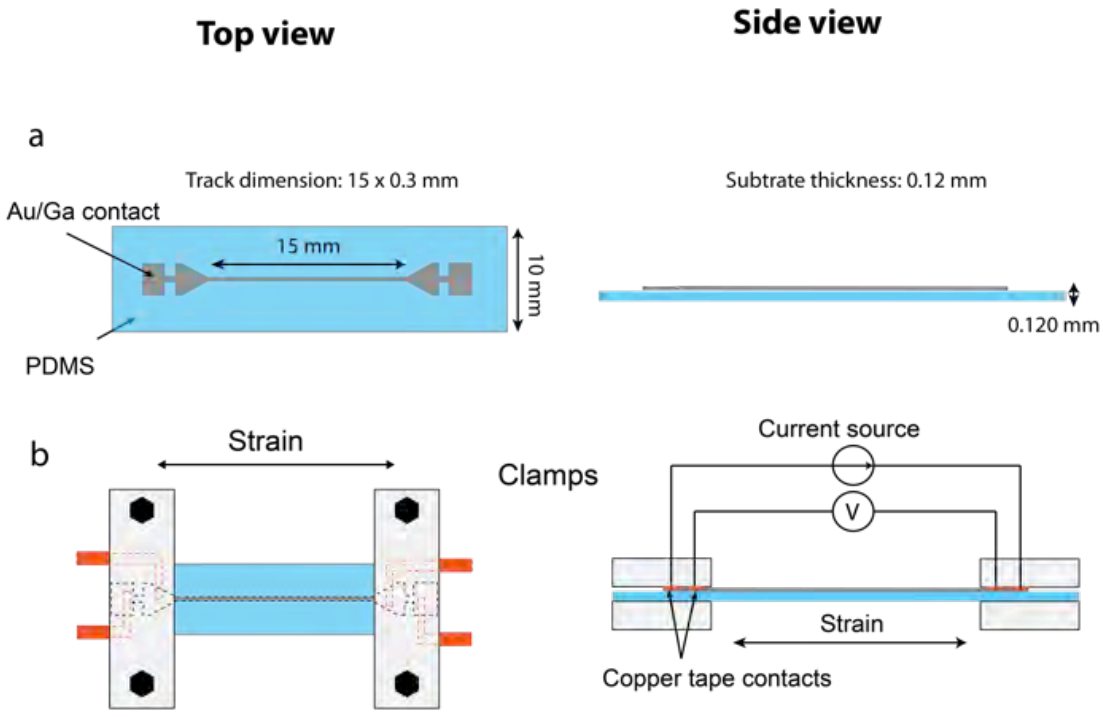

Supplementary Figure S8: Preparation of samples for electromechanical characterization. a, Top (left) and side (right) schematics of the biphasic gold-gallium thin film on a PDMS substrate used for electromechanical characterization. PDMS substrate was 120 µm thick, 30 mm long and 10 mm wide. The biphasic thin film was patterned using a stencil mask to produce 15 mm long and 0.3 mm wide conductive tracks featuring large contacts at the extremities. **b,** Top (left) and side (right) schematics of clamped samples for electromechanical characterization. Each clamp featured two contact pads that enabled constant electrical and mechanical contact with the tested sample. Resistance of the track, measured using the 4-point probes method (Keithley 2400 source-meter), and the position of the clamps were measured continuously.

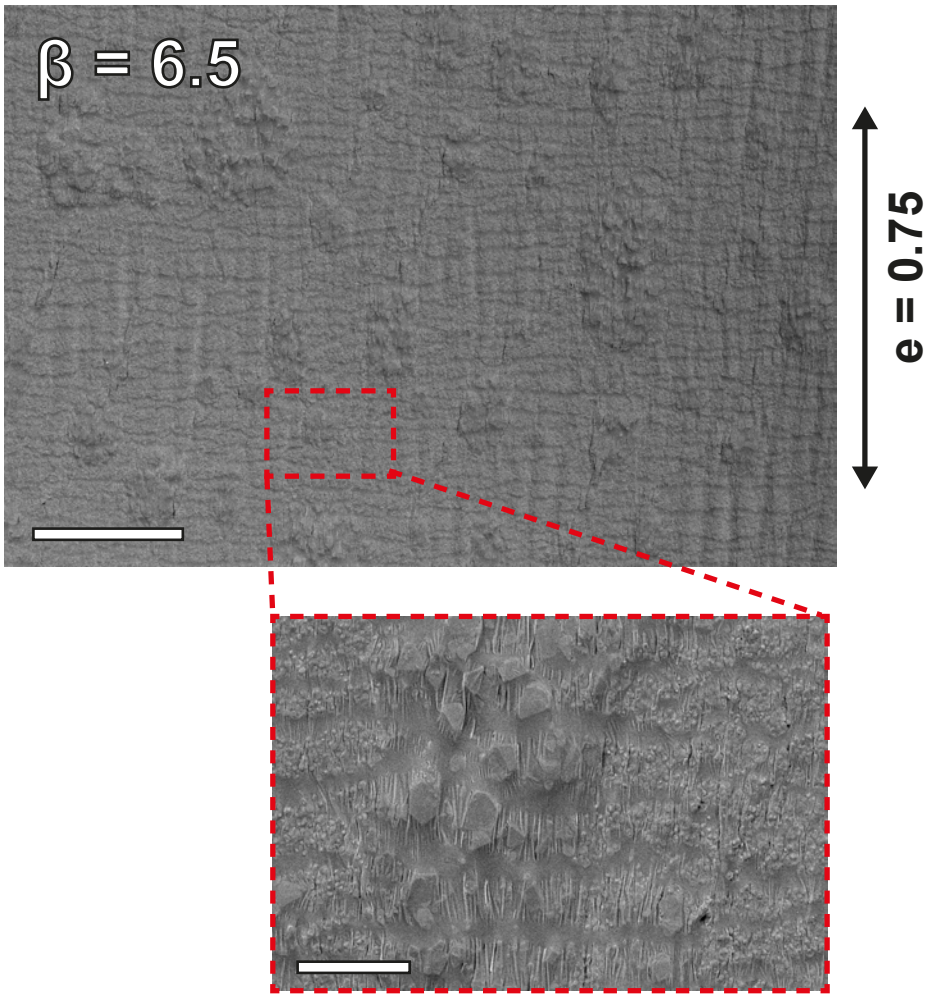

Supplementary Figure S9: SEM images of a biphasic gold-gallium thin film on PDMS substrate (β = 6.5) under 0.75 applied uniaxial mechanical strain. The film remains continuous and no cracks are observed. Scale bar is 20 µm on main image and 5 µm on the magnification.

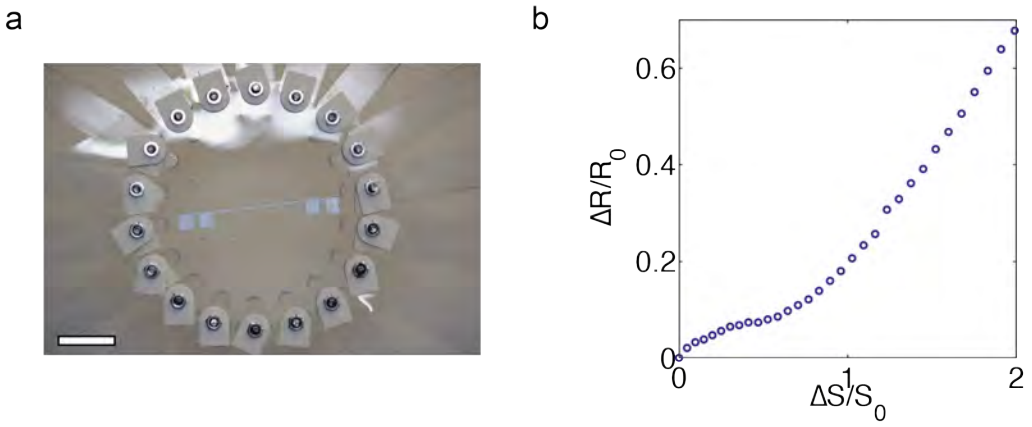

Supplementary Figure S10: Radial stretching of the biphasic gold-gallium thin films conductors on a PDMS substrate. **a,** Picture of a 35 mm × 0.5 mm track in the radial stretcher.[R1] Scale bar is 20 mm. **b,** Relative increase in resistance of the track was measured using the four point probe measurement method as a function of the relative increase in surface area of the support membrane.

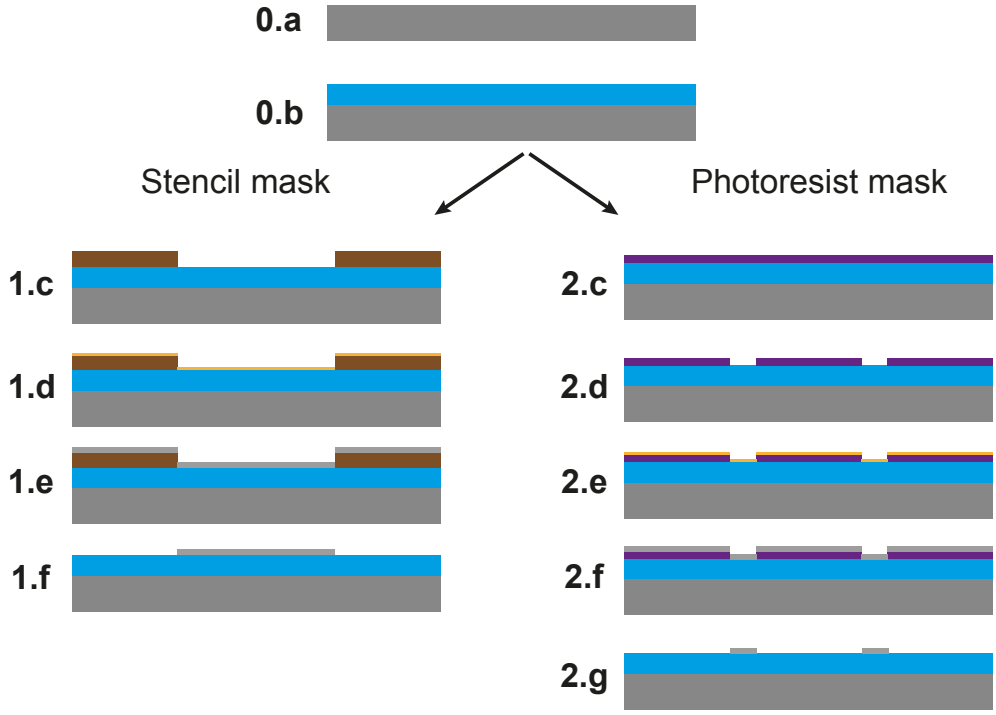

Supplementary Figure S11: Process flow for patterning biphasic gold-gallium thin films using stencil or photoresist masks. **0.a**, Exposure of silicon or glass wafer to oxygen plasma and coating with a self-assembled layer of trichloro(1H,1H,2H,2H-perfluorooctyl)silane. **0.b**, Spin-coating of PDMS and curing at 80 °C for at least 2 hours. **1.c,** Lamination of polyimide stencil mask. **1.d,** Gold sputtering. **1.e,** Gallium thermal evaporation. **1.f,** Stencil mask removal **2.c,** Photoresist spin-coating. **2.d,** Exposure and development of PR. **2.e,** Gold sputtering. **2.f,** Gallium thermal evaporation. **2.g,** Lift-off.

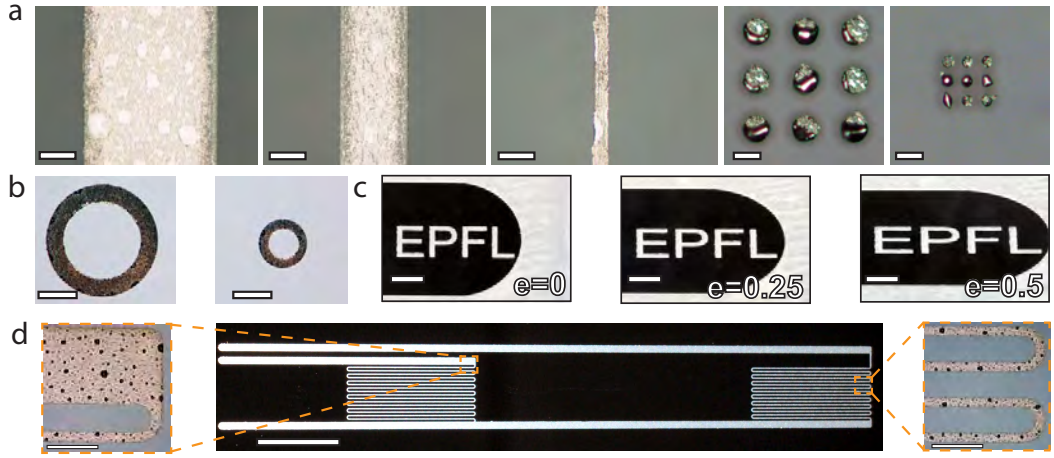

Supplementary Figure S12: Micropatterning of biphasic gold-gallium conductors on PDMS substrates with lift-off processing. **a,** Optical microscope images of (left to right) 100 µm, 50 µm, and 10 µm wide tracks and 3 x 3 matrices of 25 µm and 10 µm dots of biphasic thin films patterned with a photolithographic lift-off process. Scale bar: 25 µm. **b-c,** Arbitrary patterns of biphasic gold-gallium thin films on PDMS substrates. Scale bars: 250 µm (b) and 1 mm (c). **d,** Pictures of patterns developed over large-area surfaces. Scale bars: 10 mm (main picture) and 500 µm (insets).

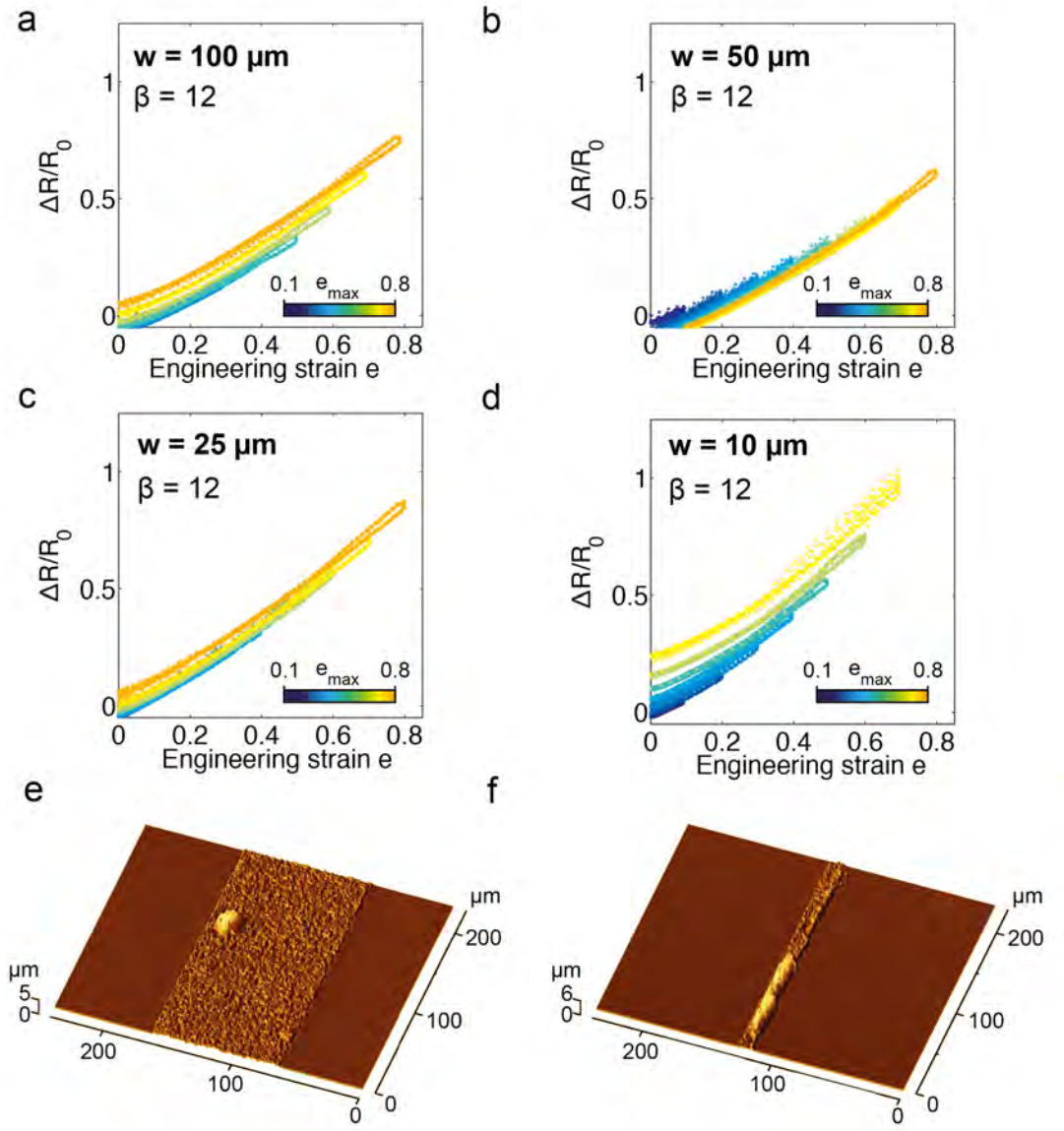

Supplementary Figure S13: Electromechanical characterization of biphasic gold-gallium tracks patterned using photolithography. a-d, Relative resistance change during incremental stretching of a 100 µm x 15 mm, 50 µm x 15 mm, 25 µm x 15 mm, and 10 µm x 15 mm biphasic gold-gallium tracks measured using the four point probe method described in Supplementary Fig. 8. Initial sheet resistances were 0.8 Ω , /sq, 0.7 Ω ,/sq, 0.6 Ω /sq and 0.4 Ω/sq, respectively. **e**, 3D reconstruction of a portion of a 100 µm wide track from white light interferometry measurements. **f**, 3D reconstruction of a portion of a 10 µm wide track from white light interferometry measurements.

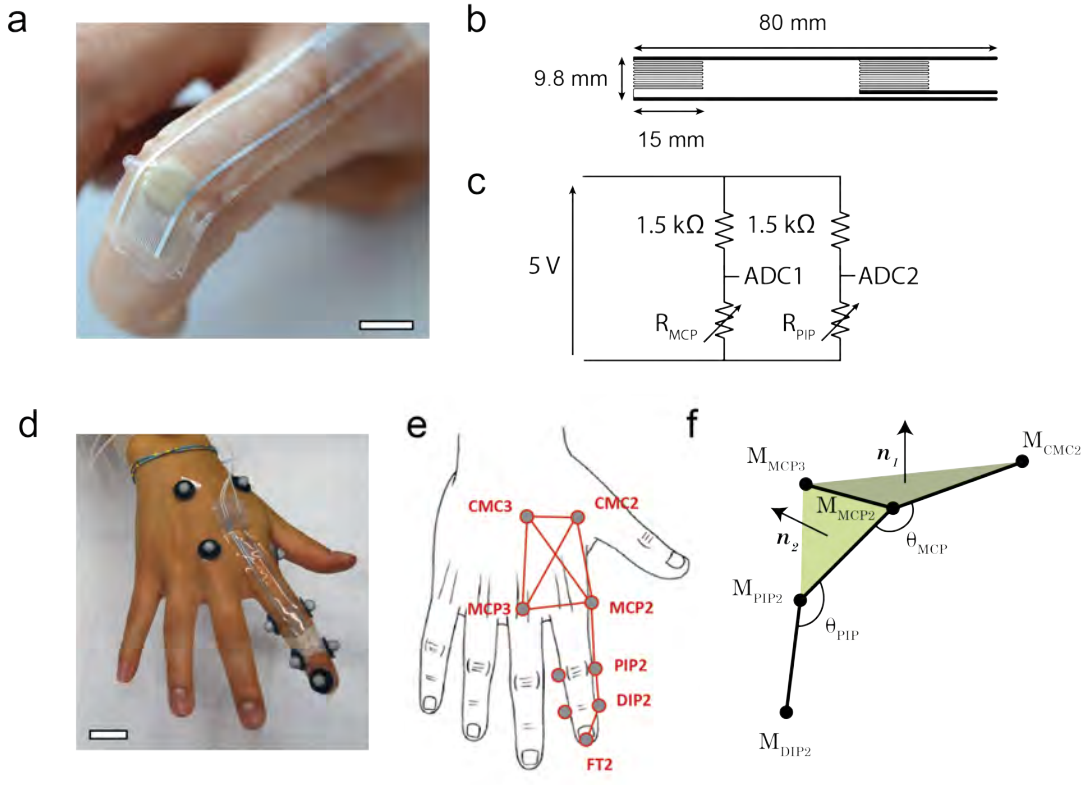

Supplementary Figure S14: Epidermal flexion sensors prepared with biphasic gold-gallium thin films. **a,** Soft strain sensors glued on the skin of the subject using silicone glue. Scale bar is 10 mm. **b,** Design of the sensors. Connection tracks are 800 µm wide and serpentine tracks are 100 µm wide. **c,** Sensing circuit. **d,** Picture of the hand of the subject equipped with the soft sensors and markers for motion capture system. Scale bar is 10 mm. **e,** Identification of the markers. Two unidentified markers were placed on the PIP2 and DIP2 joints for redundancy and were not used in this study. **f,** Geometrical representation of the markers used for the calculation of the θ_{MCP} and θ_{PIP} angles.

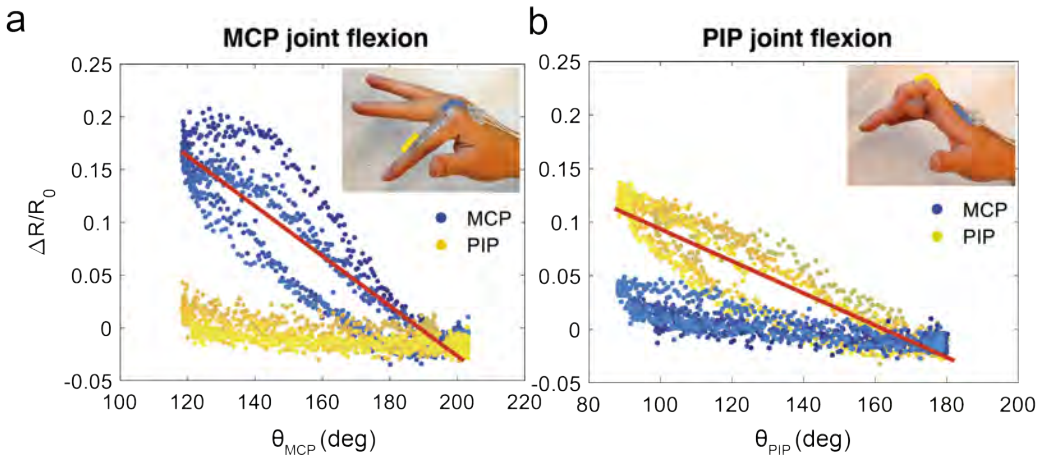

Supplementary Figure S15: Calibration of epidermal flexion sensor using the motion capture system. a, Relative increase in resistance in the strain gauges place over the MCP and PIP joints as a function of the MCP angle θ_{MCP} computed using the motion capture system. The subject was asked to flex only the MCP joint, as shown in inset picture. Red line represents linear fit of the response of the gauges placed over the MCP joint ($R^2 = 0.86$). **b,** Relative increase in resistance of the strain gauges placed over the MCP and PIP joints as a function of the PIP angle θ_{PIP} computed using the motion capture system. The subject was asked to flex only the PIP joint, as shown in inset picture. Red line represents linear fit of the response of the gauge placed over the PIP joint ($R^2 = 0.87$).

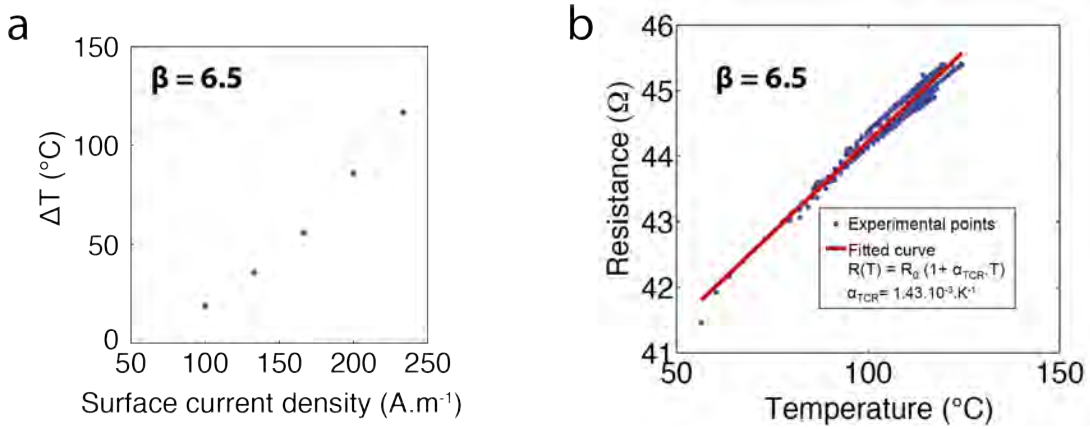

Supplementary Figure S16: Thermal properties of self-heated (Joule effect) biphasic gold-gallium thin films on PDMS substrates. Elevation of temperature in a self-heated gold-gallium thin film track (β = 6.5) on PDMS substrate as function of the surface current density in the track. **b,** Resistance of a self-heated biphasic gold-gallium track as function of temperature of the track. The temperature coefficient of resistance ($1.43\ 10^{-3}\ K^{-1}$) was extrapolated from linear regression.

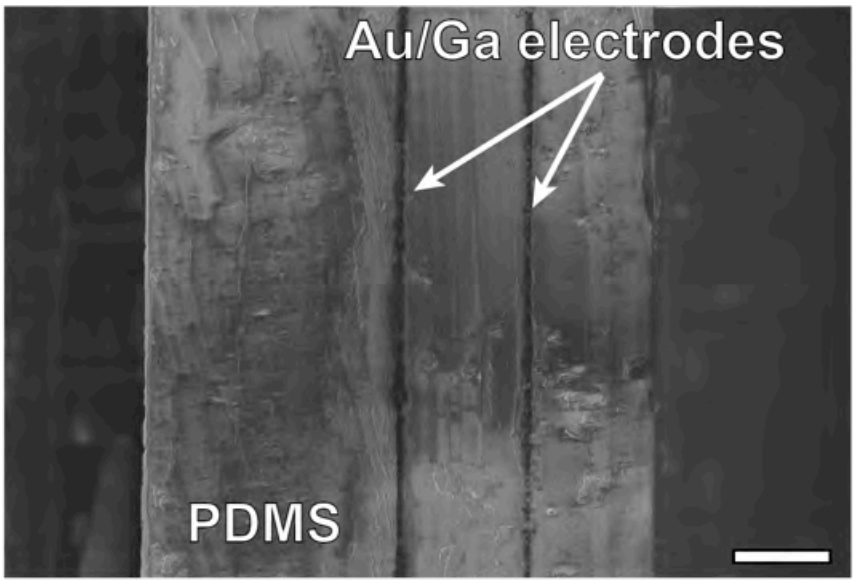

Supplementary Figure S17: SEM image of the cross section of a dielectric elastomer actuator cantilever prepared with PDMS and biphasic gold-gallium thin film electrodes. Scale bar is 20 μm.

2. Supplementary Methods

Materials characterization methods

Energy dispersive spectroscopy (Fig. 2, Fig. S6)

Energy dispersive spectroscopy (EDS) data were acquired in the Merlin SEM at beam energy of 20 keV, using a 50 mm^2 X-Max silicon drift detector from Oxford Instruments and analyzed using Aztec software from same supplier.

Edge roughness measurement

The root mean square (RMS) edge roughness of the lines patterned by lift-off was derived from a series of optical microscope images using the Analyze_Stripes macro for ImageJ.[R2]

Sample preparation for cross-section observation (Fig. 1b)

Samples were prepared on a 120 µm thin PDMS substrate on a silicon wafer. We peeled off a sample from the wafer and put a solid gallium crystal in contact with the film to initiate crystallization of liquid gallium. Then we immersed the sample in liquid nitrogen to cool it below the glass transition temperature of PDMS (-125 °C). We initiated a crack on the side of the sample using scissors and eventually broke it in two parts using tweezers.

Sample imaging under uni-axial stretch in the SEM (Fig. 3, Fig. S9)

The samples were cut, peeled from their carrier wafer and mounted on a manual aluminum uni-axial stretcher. Controlled strain was applied to stretch the soft samples to a strain e. The samples in the stretcher were loaded into the SEM chamber and subsequently imaged using identical parameters to those selected for (unstrained) samples imaged on carrier wafers.

Electromechanical characterization of the biphasic gold-gallium thin film conductors on soft substrates (Fig. 3, Fig. S2, S8, S10, S13)

Three different metrics were extrapolated from the experimental data to characterize the electromechanical response of the film, as follows:

- the initial sheet resistance

$$R_S = R_0 \frac{l}{w}$$

where R_0 is the initial resistance of the sample (before stretching) ; l and w are the length and width of the conductive tracks, respectively.

- the relative change of resistance after cycling at 0.5 strain

$$\frac{\Delta R_0^{0.5}}{R_0} = \frac{R_0^{0.5} - R_0}{R_0}$$

where $R_0^{0.5}$ is the measured resistance at 0 strain after the sample has been stretched 20 times to 0.5 strain; R_0 is the initial resistance of the conductor.

- the gauge factor GF defined as the slope of the relative change of resistance as a function of the applied strain, and computed using a linear fit on the last cycle at 0.5 maximal applied strain.

Extremely large deformation on a polyurethane substrate (Fig. 3e)

A biphasic gold-gallium thin film was deposited on a 250 µm thick polyurethane foam substrate (Coveris Inspire 7250). Conductors were patterned with stencil lithography as described above. Ten samples were stretched to an applied strain of 4, or electrical failure.

Integration of surface mounted LEDs (Fig. 1,4)
Biphasic gold-gallium thin film conductors were patterned on PDMS substrates using stencil masks. Drops of eutectic gallium indium (EGaIn, Sigma–Aldrich) were deposited on the contact pads of the circuits to form small bumps. Surface mounted LEDs (0402, Everlight Electronics) were manually placed and secured with a drop of room temperature vulcanization silicone (734 flowable sealant, Dow Corning). Next, the assembly was coated with a 100 μm thick encapsulating PDMS film and cured at 80 °C for two hours.

Multilayered conductor network prepared with biphasic gold-gallium thin films and PDMS (Fig. 1,4)
The soft assembly consisted of two PDMS-biphasic conductors membranes. The bottom membrane was a 100 μm thick PDMS substrate metalized with the biphasic conductors using stencil patterning as described above. The top membrane was prepared on a 5 mm thick, 4" wafer sized slab of PDMS. The slab's surface was functionalized with a 1H,1H,2H,2H-perfluorooctyltriethoxysilane (Sigma-Aldrich) release monolayer under weak vacuum. A 100 μm thick PDMS layer (top layer) was then spin-coated on the PDMS slab and cured. Using a hole puncher (Technical Innovations), the top layer was punctured at locations corresponding to the sites of the vias and further metalized using stencil patterning as previously described. The top layer was then peeled-off from the PDMS slab, plasma activated (29 W, 20 s, PDC-32G-2 etcher, Harrick Plasma), aligned and bonded to the bottom membrane. Drops of eutectic gallium indium (EGaIn, Sigma–Aldrich) were then deposited in the vias to form a conductive bond between the two metallized membranes. The soft assembly was next spin-coated with a 100 μm thick PDMS encapsulation layer and cured at 80°C for two hours.
We used this approach to prepare a stretchable matrix of 4 x 4 green LEDs interconnected with two planes of biphasic conductors. Powering of the LEDs is controlled and sequenced using an Arduino board. The circular membrane was clamped to a rigid frame through which pressurized air was cycled thereby inflating / releasing the soft optoelectronic skin (Fig. 1 and Supplementary Movie 1).

Thermal properties of self-heated (Joule effect) Au/Ga thin film (Fig. S16)
Biphasic gold-gallium thin film conductors ($\beta = 6.5$) were prepared and clamped in the uni-axial stretcher. Electrical resistance and current running through of the conductor were measured using a 4-point probes method (2400 source-meter, Keithley) and acquired synchronously at 3.8 Hz on a computer running a custom LabVIEW program (Fig. S8). In parallel, a thermal camera (A325 sc, FLIR systems) and close up lens (1x 25 μm, FLIR systems) were used to monitor synchronously the temperature at the surface of the samples (sampling rate: 5.6 Hz).

Fabrication, mounting and characterization of finger flexion sensors (Fig. S14, S15)
Flexion sensors were embedded on a 100 μm thick PDMS membrane and patterned with lift-off. The soft stipe was adhered and secured on the index of a subject using silicone glue (7-9700 Soft Skin Adhesive from Dow Corning). The width of the biphasic interconnects and serpentine sensors were 800 μm and 100 μm (8 serpentines per sensor), respectively.
The resistance variation of each sensor was recorded through a voltage divider (Suppl. Fig. 13c) at 1 kHz with a 16-bit resolution.
We used a motion capture system composed of eight Bonita B10 cameras from Vicon and the associated Nexus software from same supplier. The system tracked markers with a precision of 0.5 mm in translation and 0.5° in rotation.

Nine markers were positioned on the carpo-metacarpal (CMC), metacarpo-phalangeal (MCP), proximal-interphalangeal (PIP) and distal interphalangeal (DIP) joints and fingertip (FTP) of the subject (Suppl. Fig. 13d). The 3D spatial position of the markers was recorded at 100 Hz. Acquisition of signals from the flexion sensors and the tracking system were synchronized.

Fabrication and evaluation of a dielectric elastomer actuator with biphasic gold-gallium thin film electrodes (Fig. S17, Supplementary Movie 3)

The soft assembly consisted of two PDMS-biphasic conductor membranes. The bottom and middle PDMS membranes were 80 μm and 20 μm thick, respectively, metallized with biphasic conductors using stencil patterning, as described above. The top 20 μm thick PDMS membrane was used for encapsulation. The bottom and middle layers were plasma activated (29 W, 20 s, PDC-32G-2 etcher, Harrick Plasma), aligned and bonded to each other, followed by the similar activation and bonding of the middle and top layers.

Actuators were powered with a high voltage source (Series FC, Glassman High Voltage Inc.) in constant voltage mode. The voltage was increased from 0 to 3,000 V in 500 V steps with a photograph recorded at each step. Displacements were measured through examination of the sequence of images in ImageJ.

Fabrication and evaluation of soft tactile sensors (Supplementary Movie 4)

Capacitive tactile sensors were prepared with biphasic gold-gallium ($\beta = 13$) electrodes and two shielding planes processed on 20 μm thick PDMS membranes. The total thickness of the soft structure was 80 μm. The soft membrane hosting 8 tactile sensors (5 x 5 mm^2 in surface area), was mounted on a acrylonitrile butadiene styrene (ABS) ring. The sensors were interfaced with a miniaturized PCB as previously reported.[R3]

3. Supplementary note

Calculation of the angular position of the phalanx using the camera tracking system and the epidermal sensors

The angle of the MCP joint was derived from the position of the markers identified in Suppl. Fig. 13e. We applied the following method to compute the angular position of the finger from the 3D spatial position of the markers. We started by projecting the points M_{CM2}, M_{MCP2} and M_{PIP2} on the plane orthogonal to the plane containing M_{CMC2}, M_{MCP2} and M_{MCP3} and itself containing M_{MCP3}. The intermediate angle value $\theta^*_{MCP} \in [0;\pi]$ was computed as:

$$\theta^*_{MCP} = atan2(\|\boldsymbol{P_{MCP2}P_{CMC2}}\times\boldsymbol{P_{MCP2}P_{PIP2}}\| , \boldsymbol{P_{MCP2}P_{CMC2}}\cdot\boldsymbol{P_{MCP2}P_{PIP2}})$$

where *atan2* is the four quadrant inverse tangent and points P are the projection of the corresponding points M having the same index.
Finally, we computed $\theta_{MCP} \in [0;2\pi]$ by looking at the sign of the dot product of the vector $\boldsymbol{M_{MCP2}M_{CMC2}}\cdot\boldsymbol{n_1}$, with the vector $\boldsymbol{n_1}$ orthogonal to the plane containing M_{CMC2}, M_{MCP2} and M_{MCP3} and itself containing M_{MCP3}:

$$\theta_{MCP} = \begin{cases} \theta^*_{MCP} & if\ \boldsymbol{M_{MCP2}M_{CMC2}}\cdot\boldsymbol{n_1} \le 0 \\ 2\pi - \theta^*_{MCP} & if\ \boldsymbol{M_{MCP2}M_{CMC2}}\cdot\boldsymbol{n_1} \ge 0 \end{cases}$$

The same scheme was applied to compute θ_{PIP}, this time using the plan containing M_{CM3}, M_{MCP2} and M_{PIP2} as a reference for the projection and final determination of the angle.
In order to calibrate the soft strain sensors, the subject was asked to sequentially move one joint at a time (Suppl. Fig. 14). The response of the MCP sensor (resp. PIP) as a function of θ_{MCP} (resp. θ_{PIP}) was used to estimate the coefficients of a linear model:

$$\frac{\Delta R_{MCP}}{R_{0,MCP}} = \alpha_{MCP}\theta_{MCP} + \beta_{MCP}$$
$$\frac{\Delta R_{PIP}}{R_{0,PIP}} = \alpha_{PIP}\theta_{PIP} + \beta_{PIP}$$

Once $\alpha_{MCP}, \beta_{MCP}, \alpha_{PIP}$ and β_{PIP} were determined, the angles of both joints could be computed from the output of the epidermal sensors.

References

_[R1] S.E. Schausberger, R. Kaltseis, M. Drack, U.D. Cakmak, Z. Major, S. Bauer, *IEEE Access* **2015**, 556.

_[R2] J.R. Bickford, "Analyse_Stripes", **2013** http://imagejdocu.tudor.lu/doku.php?id=macro:analyze_stripes

_[R3] A.P. Gerratt, H.O. Michaud, S.P. Lacour, *Advanced Functional Materials* **2015**, *25*, 2287.

4. List of Supplementary Movies

Supplementary Movie 1: Stretchable hybrid arrays of light emitting diodes interconnected with a network of biphasic solid-liquid conductors

Supplementary Movie 2: Epidermal flexion sensor skin

Supplementary Movie 3: Voltage-controlled actuation of a dielectric elastomer actuator with biphasic gold-gallium thin film electrodes

Supplementary Movie 4: Soft capacitive touch sensor array on PDMS membrane